

Halperin-Saslow modes as the origin of the low-temperature anomaly in NiGa₂S₄

Daniel Podolsky¹ and Yong Baek Kim^{1,2}

¹*Department of Physics, University of Toronto, Toronto, Ontario, Canada M5S 1A7*

²*School of Physics, Korea Institute for Advanced Study, Seoul 130-722, Korea*

(Received 2 March 2009; published 3 April 2009; publisher error corrected 2 June 2010)

The absence of magnetic long-range order in the triangular lattice spin-1 antiferromagnet NiGa₂S₄ [S. Nakatsuji *et al.* Science **309**, 1697 (2005)] has prompted the search for a novel quantum ground state. In particular, several experiments suggest the presence of a linearly dispersing mode despite no long-range magnetic order. We show that the anomalous low-temperature properties of NiGa₂S₄ can naturally be explained by the formulation developed by Halperin and Saslow [Phys. Rev. B **16**, 2154 (1977)] where the linearly dispersing Halperin-Saslow mode may exist in the background of frozen spin moments and zero net magnetization. We provide consistency checks on the existing experimental data and suggest future experiments that can further confirm the existence of the Halperin-Saslow mode. Our results place important constraints on any microscopic theory of this material.

DOI: [10.1103/PhysRevB.79.140402](https://doi.org/10.1103/PhysRevB.79.140402)

PACS number(s): 75.50.Ee, 75.10.-b, 75.25.+z, 75.50.Lk

I. INTRODUCTION

Frustrated magnets are an excellent playground for the discovery of novel quantum phases of matter. The intricate interplay between geometrical frustration and quantum fluctuations lies at the heart of the physical mechanism for such possibilities. Recently, various frustrated magnets with small spin ($S=\frac{1}{2}$ and $S=1$) have been discovered.^{1,2} These experiments provide great opportunities for studying quantum as well as thermal fluctuation effects in frustrated magnets. In particular, NiGa₂S₄ is an insulator composed of spin-1 Ni atoms on a triangular lattice, which shows no long-range magnetic order in neutron scattering down to at least 0.35 K, despite an antiferromagnetic Curie-Weiss temperature $|\Theta_{\text{CW}}|=80$ K.¹ Instead, spin freezing is observed at $T_f=8$ K, a temperature that also serves as the onset for a variety of unusual experimental signatures.^{3,4}

Below T_f , the spin susceptibility saturates to a constant value, while the magnetic part of the specific heat acquires a T^2 power law.¹ This T^2 dependence of the specific heat is consistent with the presence of gapless hydrodynamic modes propagating in two dimensions, provided that these modes are coherent over a length scale L_0 that exceeds 500 lattice spacings.¹ On the other hand, elastic neutron scattering on powder¹ and single crystal⁵ samples show no evidence of long-range magnetic order. Instead, coincident with the spin freezing temperature, there is the onset of *static, yet short-range* magnetic correlations, with a correlation length ξ of order of only seven lattice spacings. In addition, nuclear magnetic resonance (NMR) measurements have observed a spin-lattice relaxation rate $1/T_1 \propto T^3$ for $T \ll T_f$.⁶ Recent inelastic neutron-scattering measurements observe a linearly dispersing excitation mode.⁵

In order to account for some of these results, there have been recent proposals of the formation of subtle types of long-range spin ordering. Based on models with large biquadratic interactions, Tsutetsugu and Arikawa⁷ proposed a three-sublattice nematic state and Bhattacharjee *et al.*⁸ proposed a uniform nematic state (see also Ref. 9 for related theoretical models). On the other hand, Kawamura and Yamamoto proposed a state with bound Z_2 vortices.¹⁰ The nematic states of Refs. 7 and 8 may be consistent with the

constant spin susceptibility, and also contain gapless director modes, which can account for the T^2 specific heat. However, these proposals leave a few questions unanswered. For instance, there is no clear connection between the onset of nematic order and the appearance of static short-range magnetic correlations seen at T_f . In addition, a nematic state does not account for the linearly dispersing inelastic neutron-scattering peak—the director modes of a nematic do not couple directly to neutrons.⁹ In this Rapid Communication, we argue that these experimental discoveries can be explained by the presence of gapless Halperin-Saslow (HS) modes.¹¹ Halperin and Saslow originally proposed the existence of hydrodynamic modes in the context of spin glasses. However, as discussed below, HS modes can exist in a much broader class of materials. HS modes have a linear dispersion, and they couple directly to atomic spins and also to neutrons. Therefore, they can account for the full phenomenology of NiGa₂S₄ in a natural way. In the rest of the paper, we will provide various qualitative and semiquantitative consistency checks, and also discuss future experimental consequences of the HS scenario. We are not aware of any confirmed example of the HS modes, therefore NiGa₂S₄ may present the first clear case for these long-sought low energy modes. Our discussion will be phenomenological in nature, as it will not address the microscopic mechanism by which the system chooses the underlying state supporting the HS modes, but will rather rely on general hydrodynamic considerations. This has the advantage that our results are not limited to NiGa₂S₄, but are easily adapted to other potentially relevant frustrated magnets.

II. OVERVIEW OF THE HALPERIN-SASLOW THEORY

Halperin and Saslow showed that a system with static moments can support low-energy hydrodynamic modes, even in the absence of periodic long-range magnetic order.¹¹ Their formalism is very general and relies on two assumptions only: the presence of static moments in the (possibly metastable) ground state, and a finite spin stiffness to slow spatial deformations of the static spin texture. If the moments are noncollinear and have zero net magnetization, the HS

theory predicts the existence of three linearly dispersing hydrodynamic modes. The elastic neutron-scattering experiments in NiGa₂S₄ indicate that there are static helical spin textures at temperatures below T_f . The fact that these spin textures are short ranged is inconsequential to the HS scenario, provided that a finite spin stiffness survives at long distances.

For a system satisfying these assumptions, the free-energy cost of a weakly perturbed state is¹¹

$$\Delta F[\mathbf{m}, \theta] = \frac{d}{2} \sum_{\alpha=1}^3 \int d^2r [m_\alpha^2 \chi^{-1} + \rho_s (\nabla \theta_\alpha)^2]. \quad (1)$$

Here χ is the spin susceptibility, ρ_s is the spin stiffness, $m_\alpha(r)$ is the local magnetization density, and θ_α are locally defined rotation angles that describe the deformation in the excited-state spin configuration. In Eq. (1) we have assumed that the system is composed of weakly coupled layers of thickness d . The variables m_α and θ_α satisfy the commutation relations $[\theta_\alpha(r), \theta_\beta(r')] = 0$ and

$$[m_\alpha(r), m_\beta(r')] = i\gamma\hbar \delta(r-r') \epsilon_{\alpha\beta\gamma} m_\gamma(r), \quad (2a)$$

$$[\theta_\alpha(r), m_\beta(r')] = i\gamma\hbar \delta(r-r') [\delta_{\alpha\beta} + \epsilon_{\alpha\beta\gamma} \theta_\gamma(r)], \quad (2b)$$

where $\gamma = g\mu_B/\hbar$ is the gyromagnetic ratio. Equation (2a) identifies the magnetization m_α as the generator of rotations, while Eq. (2b) states that m_α and θ_α are canonically conjugate variables, together with the fact that θ_α transforms as a vector under rotations.

We obtain the Heisenberg equations of motion for m_α and θ_α using Eqs. (1) and (2). These yield three degenerate polarizations of spin waves with dispersion $\omega_k = vk$, with velocity $v = \gamma\sqrt{\rho_s/\chi}$. More generally, χ and ρ_s are tensors, leading to three nondegenerate spin waves, with polarization-dependent velocities $v_j = \gamma\sqrt{\rho_j/\chi_j}$.

III. BASIC CONSIDERATION: CONTRASTING SPECIFIC HEAT AND ELASTIC NEUTRON-SCATTERING DATA

The presence of gapless HS modes is consistent with the T^2 specific heat in NiGa₂S₄. For linearly dispersing modes in two dimensions,

$$\frac{c_M}{N_A \nu} = \frac{3\zeta(3)}{\pi d} \frac{k_B^3 T^2}{\hbar^2} \sum_j \frac{1}{v_j^2} - \frac{3k_B \pi}{L_0^2 d}. \quad (3)$$

Here, $\zeta(3) = 1.202\dots$, N_A is Avogadro's number, the sum runs over polarizations j , v_j is the collective-mode velocity, and $\nu = \sqrt{3}a^2 d/2$ is the volume of a unit cell, where we have assumed decoupled layers of thickness d and a is the in-plane lattice spacing. Here, we have allowed for the possibility that the collective modes are coherent only up to some length scale L_0 . Experimental fits yield a lower bound, $L_0 > 500a$.¹

The HS modes correspond to the elastic deformations of an order parameter, hence they are well defined to the lowest energies or even in the hydrodynamic limit. The modes become sharper at higher energies or in the collisionless regime

due to a lack of scattering. Since the real part of the dispersion is the same in the hydrodynamic and collisionless regimes,¹¹ the specific heat shows the same temperature dependence in both cases, leading to no noticeable change across two regimes.

Elastic neutron-scattering measurements show that the freezing temperature T_f coincides with the onset of static short-range-ordered moments. Peaks appear at an incommensurate wave vector $\mathbf{Q} = (1/6 - \epsilon, 1/6 - \epsilon)$. The peaks are static, but they are broad in momentum, corresponding to short-range order over a length $\xi_{xy} \sim 7a$ in plane, and $\xi_z \sim 6 \text{ \AA}$ out of plane. The moments arrange in a helical pattern. This wave vector and spin structure are expected from a system with a weak ferromagnetic nearest-neighbor coupling and a large antiferromagnetic third-nearest-neighbor coupling, $J_3 \gg -J_1 > 0$, which is consistent with semiempirical cluster calculations.¹² A large $J_3 > 0$ is also supported by *ab initio* calculations.¹³

The correlation length ξ_{xy} is much smaller than the scale L_0 , i.e., the collective modes responsible for the T^2 specific heat exist over a much larger length scale than the helical regions seen in neutron scattering. Here we explore the possibility that below T_f , the system is in a quantum spin-glass-like state composed of helical domains that do not order at long distances, yet have a finite spin stiffness. We may think of each helical domain as some block degree of freedom. The residual interaction between blocks, of order T_f , is frustrated and disordered, leading to freezing behavior at T_f and the absence of long-range helical order. Precisely how such a state is formed may require understanding of microscopic details such as the role of quantum $S=1$ moments. Independently of the underlying mechanism, however, we focus on the generic properties that follow from the hydrodynamics of such a system.

IV. TWO ENERGY SCALES FROM THE SUSCEPTIBILITY AND SPECIFIC HEAT

As a first semiquantitative check, we would like to know whether the magnitude of the low-temperature susceptibility and specific-heat anomaly are consistent with the HS scenario. Here these two quantities are related through the spin stiffness ρ_s , since $c_M/T^2 \propto 1/\nu^2 \propto \chi_M/\rho_s$. From χ_M and c_M/T^2 , we can extract two energy scales,

$$E_1 = \frac{2g^2 \mu_B^2 S(S+1)}{z\chi_M/N_A} = k_B(113 \text{ K}), \quad (4)$$

$$E_2 = \frac{3n_p \zeta(3)}{\pi} \frac{k_B^3}{g^2 \mu_B^2 c_M/T^2} = k_B(6.5 \text{ K}), \quad (5)$$

where $z=6$ is the coordination number of the lattice, and $n_p=3$ is the number of degenerate hydrodynamic modes. Above, we have used the experimentally measured values, $\chi_M(T \rightarrow 0) = 0.0089 \text{ emu/mole}$ and $c_M/T^2 = 2.6 \times 10^{-2} \text{ J mole}^{-1} \text{ K}^{-3}$.¹

The energy E_1 is related to the effective interaction between a spin and its environment, whereas E_2 corresponds to the spin stiffness extracted from measurements. Note that,

while E_1 is comparable to the microscopic energy scale $|\Theta_{\text{CW}}|=80$ K, E_2 is much smaller. This is consistent with the HS scenario: the stiffness is expected to be considerably renormalized relative to the microscopic energies, to a scale of order of the freezing temperature $T_f=8$ K.

We can provide a theoretical upper bound on the spin stiffness. This is done by computing the spin stiffness of a long-range-ordered helical state, ignoring the fact that spin correlations in NiGa_2S_4 are short ranged. Carrying out an analysis similar to Ref. 11,

$$\rho_{\alpha\beta}^{\text{max}} = -\frac{1}{2V}(\delta_{\alpha\beta} + \delta_{\alpha,3}\delta_{\beta,3})\sum_{\vec{\mu}} J_{\vec{\mu}}\mu_x^2\sum_i \langle \mathbf{S}_i \cdot \mathbf{S}_{i+\vec{\mu}} \rangle, \quad (6)$$

where the sum runs over all vectors $\vec{\mu}$ connecting lattice sites, $\mu_x = \vec{\mu} \cdot \hat{x}$ for an arbitrary direction \hat{x} , and V is the volume of the sample. Equation (6) is an upper bound on the stiffness of NiGa_2S_4 , since it assumes an elastic deformation of the spin texture that is uniform across the sample. On the other hand, in the real material with disorder, it pays off to put the bulk of the deformation across weak links. Since the helical spin correlations in NiGa_2S_4 have wave vector near $\mathbf{Q}=(1/6, 1/6)$, Eq. (6) gives the upper bound,

$$\rho_{zz}^{\text{max}} = 2\rho_{xx}^{\text{max}} = 2\rho_{yy}^{\text{max}} \approx 4\sqrt{3}J_3\langle S_i^2 \rangle/d, \quad (7)$$

Using $|\Theta_{\text{CW}}|=80$ K and the ratio¹ $J_1/J_3=-0.2$, we obtain $J_3 \approx k_B(25$ K). Plugging in the experimental values,¹ $g=2$, $\langle S_i^2 \rangle \approx 0.75$, we obtain an upper bound, $\rho_{xx}^{\text{max}}d = k_B(49$ K), which is indeed larger than E_2 . Conversely, we get a lower bound $c_M/T^2 > 2.9 \times 10^{-3}$ J mole⁻¹ K⁻³ that is consistent with the experimentally measured value, which is about nine times larger than this bound. In fact, the ratio between the two is comparable to the frustration parameter, $T_f/|\Theta_{\text{CW}}|$, which is a natural renormalization factor for the spin stiffness in a frustrated spin system.

Note that the definition of the two energy scales E_1 and E_2 is *model independent*, and can therefore be used to characterize the experiments and to compare with other theoretical proposals. As we have argued, in the HS scenario, it is natural to find $E_2 \sim T_f \ll E_1 \sim |\Theta_{\text{CW}}|$. On the other hand, for the spin nematic states of Refs. 7 and 8, this requires some fine tuning. For example, in order to obtain $E_2 \ll |\Theta_{\text{CW}}|$, the system has to be tuned to be very close to a quantum critical point.

V. EFFECT OF MAGNETIC FIELD AND SPIN ANISOTROPY

One of the salient features of NiGa_2S_4 is the weak effect of magnetic fields on the specific-heat anomaly. In a typical magnetically ordered system, external fields gap out some of the collective modes and thus suppress the specific heat below a temperature of order $T^* = g\mu_B H/k_B$.

In the presence of an external field, one must add a Zeeman coupling to the free energy, $f_Z = -g\mu_B \mathbf{H} \cdot \mathbf{m}$. The spectrum of collective modes is computed from the Heisenberg equations of motion for θ_α and m_α by taking into account Eq. (2). It turns out the second term in the commutator [Eq. (2b)] only gives anharmonic corrections that can be ignored for small amplitude spin waves.

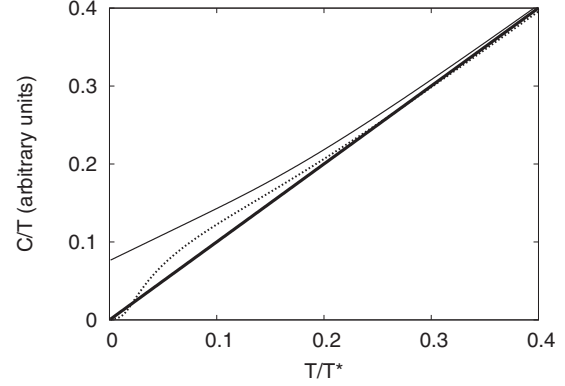


FIG. 1. Specific heat for an isotropic system (thick solid line); for an isotropic system in a magnetic field (thin solid line); and for a system with easy-plane anisotropy with $u_{\text{an}}=0.3T^*$, together with an magnetic field perpendicular to the anisotropy plane (dotted line). Here, $T^* = g\mu_B H$.

The excitation spectrum can be obtained from these equations of motion and is composed of three nondegenerate polarizations, $\omega_0 = vk$ and $\omega_{\pm} = \pm \frac{g\mu_B H}{2} + \sqrt{(\frac{g\mu_B H}{2})^2 + (vk)^2}$. Hence, ω_0 is unchanged by the magnetic field and ω_+ $\approx g\mu_B H + \frac{v^2 k^2}{g\mu_B H}$ is gapped. However, the third mode, $\omega_- \approx \frac{v^2 k^2}{g\mu_B H}$, obtains a quadratic spectrum at low energies. This soft mode compensates for the gapped mode ω_+ , so that the deviation from the T^2 anomaly is negligible down to $T \approx T^*/4$ as shown in Fig. 1. This is consistent with the weak-field dependence of the specific heat down to the lowest temperature in the experiments.

In realistic systems, anisotropy in the spin interactions will cut off the T -linear specific heat. Susceptibility measurements suggest that NiGa_2S_4 has a weak easy-plane anisotropy, which we can capture by a free energy $f_{\text{an}} = u_{\text{an}}(\theta_x^2 + \theta_y^2)$. In the absence of a magnetic field, this type of anisotropy introduces a gap in two of the three HS modes. This gap is of order u_{an} , and is likely very small in NiGa_2S_4 .

VI. NUCLEAR MAGNETIC RESONANCE

NMR measurements on ^{69,71}Ga nuclei yield a spin-lattice relaxation $1/T_1 \propto T^3$ at temperatures below 1 K.⁶ This is consistent with the HS scenario. The dissipative part of the dynamic spin susceptibility due to the HS modes is $\chi''(\mathbf{k}, \omega) = \frac{\chi_0 D k^2 \omega}{2} \left[\frac{1}{(\omega - vk)^2 + (Dk)^2} \frac{1}{(\omega + vk)^2 + (Dk)^2} \right]$ plus regular terms. For modes propagating in two dimensions, this leads to $1/T_1 \propto T^3$. Note that, even if the HS modes are gapped due to anisotropy, two-magnon Raman scattering also yields $1/T_1 \propto T^3$,¹⁴ as does two-magnon Raman scattering in a nematic state.¹⁵

VII. DIRECT DETECTION OF HS MODES VIA INELASTIC NEUTRON SCATTERING AND FUTURE EXPERIMENTS

The HS modes are spin-one excitations, and therefore couple directly to neutrons. Recent inelastic neutron-scattering measurements indeed see evidence of a linearly

dispersing mode centered at wave vector \mathbf{Q} , and with spin-wave velocity $v_{\text{neutron}}=29 \text{ meV \AA}$.⁵ On the other hand, the velocity extracted from the specific-heat anomaly via Eq. (3) is much smaller, $v_{\text{sh}}=\sqrt{n_p}5.4 \text{ meV \AA}=9.35 \text{ meV \AA}$, where we use $n_p=3$ collective-mode polarizations.

This large difference between v_{sh} and v_{neutron} is due to the fact that v_{neutron} probes the velocity of relatively high-energy spin waves. In the current measurements, the inelastic neutron peaks can only be resolved clearly for energies larger than 1 meV. These high-energy modes do not contribute directly to the specific-heat anomaly below $T_f=8 \text{ K}$. In fact, at these energies the spin waves are expected to probe the bare stiffness. An estimate for the bare stiffness tensor is the stiffness computed for the helical state, as given in Eq. (7). This yields two different spin-wave velocities, $v_{\text{helical}}^x=v_{\text{helical}}^y=24 \text{ meV \AA}$ and $v_{\text{helical}}^z=34 \text{ meV \AA}$. These velocities are consistent with current experiments—the peaks in the neutron data are very broad, and thus it may be difficult to identify two separate but nearby peaks.

Future experiments may be able to distinguish the two separate spin-wave velocities. In addition, with increased resolution it may be possible to measure the dispersion of spin waves to lower energies. In the HS scenario, this would yield a spin-wave velocity that changes with wave vector, from v_{sh} very close to \mathbf{Q} , to v_{helical} at wave vectors far from \mathbf{Q} . Hence, this would constitute a direct measurement of the length-scale dependent spin stiffness. One further signature of the HS modes that may be seen in future neutron-scattering experiments is the spin-wave damping, which is predicted to be¹¹ $\Lambda=D(\mathbf{k}-\mathbf{Q})^2$. We note that the low-energy director modes that occur in the nematic states of Refs. 7 and 8 do not couple directly to neutrons at long wavelengths,⁹ and therefore cannot account for these inelastic neutron-scattering peaks.

VIII. OTHER CONSIDERATIONS: TWO-LEVEL SYSTEMS

In conventional spin glasses, the T^2 contribution to specific heat coming from HS modes is overwhelmed by a linear T contribution coming from localized two-level systems (TLS),¹⁶ $c_{\text{TLS}}=\frac{\pi^2}{6}N_0k_B^2T$. Here, N_0 is the density of states of TLS. A rough estimate for N_0 can be obtained by assuming that the energy distribution function of a single TLS is $1/(k_B T_f)$, and that there is one TLS in each correlation volume $v_\xi \sim \xi_{xy}^2 d$. Using the in-plane correlation length $\xi_{xy} \sim 7a$, one obtains an approximate upper limit $N_0 \leq 1/$

$\xi_{xy}^2 \xi_{xz} k_B T_f$, leading to $\frac{c_{\text{TLS}}}{T} \leq 3.0 \times 10^{-2} \text{ J mol}^{-1} \text{ K}^{-2}$. If present, such a contribution would be seen only at the lowest temperatures explored in Ref. 1. This suggests that the HS modes give the dominant contributions in the temperature range studied in Ref. 1.

IX. CONCLUSION

We have shown that the phenomenology of NiGa_2S_4 below the freezing temperature T_f can naturally be explained by the Halperin-Saslow scenario. In this theory, linearly dispersing HS modes in the background of frozen spin moments can exist for a much longer length scale than that of the short-range magnetic order. This explains the simultaneous onset of the short-range helical magnetic order and T^2 specific heat at T_f . The HS modes are consistent with T^3 spin-lattice relaxation rate observed in the NMR experiments. We also showed that the specific-heat anomaly in the HS scenario is only weakly sensitive to applied magnetic field as observed in the experiments. In more recent experiments on purer samples,¹⁷ indications of freezing start to show up at 10K. However, only at 2 K do the magnetic moments seem to be completely frozen.¹⁷ Given that the freezing temperature may depend on the time scale of the probe, there might be some ambiguity associated with it, leading to some uncertainty of the value of the spin stiffness in our analysis. Notice, however, that the value of the experimentally extracted spin stiffness $E_2=6.5 \text{ K}$ is in rough agreement with both extremes of the temperature range 2–10 K.

It was pointed out that the HS modes may have already been observed in inelastic neutron scattering at relatively high energies, although current experimental resolution does not give access to the low-energy mode dispersion relation. We argued that the spin-wave velocity measured at relatively high energies reflects the bare spin stiffness and the velocity of the low energy HS modes, which is directly related to the low-temperature specific heat, should be different at lower energy scales. We provided self-consistent estimates of both the low- and high-energy spin-wave velocities. These predictions as well as the three polarizations of the spin waves and the detailed magnetic field dependence can be tested in future neutron-scattering experiments on single crystals.

We thank Y. Maeno, S. Nakatsuji, T. Senthil, and C. Stock for helpful discussions. This work was supported by the NSERC of Canada, CIFAR, CRC, and KRF-2005-070-C00044.

¹S. Nakatsuji *et al.*, *Science* **309**, 1697 (2005).

²Y. Shimizu *et al.*, *Phys. Rev. Lett.* **91**, 107001 (2003); J. S. Helton *et al.*, *ibid.* **98**, 107204 (2007); Y. Okamoto *et al.*, *ibid.* **99**, 137207 (2007).

³S. Nakatsuji *et al.*, *J. Phys.: Condens. Matter* **19**, 145232 (2007).

⁴S. Nakatsuji *et al.*, *Phys. Rev. Lett.* **99**, 157203 (2007).

⁵C. Stock *et al.* (unpublished).

⁶H. Takeya *et al.*, *Phys. Rev. B* **77**, 054429 (2008).

⁷H. Tsunetsugu *et al.*, *J. Phys. Soc. Jpn.* **75**, 083701 (2006).

⁸S. Bhattacharjee *et al.*, *Phys. Rev. B* **74**, 092406 (2006).

⁹A. Läuchli *et al.*, *Phys. Rev. Lett.* **97**, 087205 (2006).

¹⁰H. Kawamura *et al.*, *J. Phys. Soc. Jpn.* **76**, 073704 (2007).

¹¹B. I. Halperin and W. M. Saslow, *Phys. Rev. B* **16**, 2154 (1977).

¹²K. Takubo *et al.*, *Phys. Rev. Lett.* **99**, 037203 (2007).

¹³I. I. Mazin, *Phys. Rev. B* **76**, 140406(R) (2007).

¹⁴T. Moriya, *Prog. Theor. Phys.* **16**, 641 (1956).

¹⁵H. Tsunetsugu *et al.*, *J. Phys.: Condens. Matter* **19**, 145248 (2007).

¹⁶P. W. Anderson *et al.*, *Philos. Mag.* **25**, 1 (1972).

¹⁷Y. Maeno and S. Nakatsuji, private communication.